

Synchronous detection of multiple optical characteristics of atmospheric aerosol by coupled photoacoustic cavity

Hua-Wei Jin(靳华伟), Ren-Zhi Hu(胡仁志), Pin-Hua Xie(谢品华), and Ping Luo(罗平)
Citation: Chin. Phys. B, 2022, 31 (**6**): 060703. DOI: 10.1088/1674-1056/ac43ad
Journal homepage: http://cpb.iphy.ac.cn; http://iopscience.iop.org/cpb

What follows is a list of articles you may be interested in

Wide dynamic detection range of methane gas based on enhanced cavity absorption spectroscopy

Yu Wang(汪玉), Bo-Kun Ding(丁伯坤), Kun-Yang Wang(王坤阳), Jiao-Xu Mei(梅教旭), Ze-Lin Han(韩泽林), Tu Tan(谈图), and Xiao-Ming Gao(高晓明)
Chin. Phys. B, 2022, 31 (**4**): 040705. DOI: 10.1088/1674-1056/ac2484

Design of a novel correlative reflection electron microscope for in-situ real-time chemical analysis

Tian-Long Li(李天龙), Zheng Wei(魏征), and Wei-Shi Wan(万唯实)
Chin. Phys. B, 2021, 30 (**12**): 120702. DOI: 10.1088/1674-1056/ac0522

Thermal desorption characteristic of helium ion irradiated nickel-base alloy

Shasha Lv(吕沙沙), Rui Zhu(朱睿), Yumeng Zhao(赵雨梦), Mingyang Li(李明阳), Guojing Wang(王国景), Menglin Qiu(仇猛淋), Bin Liao(廖斌), Qingsong Hua(华青松), Jianping Cheng(程建平), Zhengcao Li(李正操)
Chin. Phys. B, 2020, 29 (**4**): 040704. DOI: 10.1088/1674-1056/ab7e99

Doppler radial velocity detection based on Doppler asymmetric spatial heterodyne spectroscopy technique for absorption lines

Yin-Li Kuang(况银丽), Liang Fang(方亮), Xiang Peng(彭翔), Xin Cheng(程欣), Hui Zhang(张辉), En-Hai Liu(刘恩海)
Chin. Phys. B, 2020, 29 (**2**): 020701. DOI: 10.1088/1674-1056/ab5fc3

Atmospheric N2O gas detection based on an inter-band cascade laser around 3.939 μm

Chun-Yan Sun(孙春艳), Yuan Cao(曹渊), Jia-Jin Chen(陈家金), Jing-Jing Wang(王静静), Gang Cheng(程刚), Gui-Shi Wang(王贵师), Xiao-Ming Gao(高晓明)
Chin. Phys. B, 2020, 29 (**1**): 010704. DOI: 10.1088/1674-1056/ab5ef6

Synchronous detection of multiple optical characteristics of atmospheric aerosol by coupled photoacoustic cavity

Hua-Wei Jin(靳华伟)[1,2,3,4], Ren-Zhi Hu(胡仁志)[1,†], Pin-Hua Xie(谢品华)[1,‡], and Ping Luo(罗平)[2,3,4]

[1] *Key Laboratory of Environmental Optics & Technology, Anhui Institute of Optics and Fine Mechanics, Chinese Academy of Sciences, Hefei* 230031, *China*
[2] *Institute of Environment Friendly Materials and Occupational Health, Anhui University of Science and Technology, Wuhu* 241000, *China*
[3] *State Key Laboratory of Coal Resources in Western China, Xi'an University of Science and Technology, Xi'an* 710054, *China*
[4] *Mechanical Engineering School, Anhui University of Science and Technology, Huainan* 232001, *China*

(Received 8 October 2021; revised manuscript received 10 December 2021; accepted manuscript online 16 December 2021)

Owing to the influence of sampling loss, cavity difference and detecting source, the multi-optical parameter measurement of atmospheric aerosol cannot be detected simultaneously in the same reference environment. In order to solve this problem, a new method of simultaneously detecting the aerosol optical parameters by coupling cavity ring-down spectrometer with photoacoustic spectroscopy is proposed. Firstly, the coupled photoacoustic cavity is formed by the organic fusion of the photoacoustic cavity and the ring-down cavity. Secondly, the integrated design of the coupling spectroscopy system is carried out. Finally, the extinction coefficient and absorption coefficient of aerosol are measured simultaneously by the system, and then the aerosol scattering coefficient and single albedo are calculated indirectly. The accuracy of the system is verified by comparing with the data from the environmental quality monitoring station, which provides a new idea for the detection of multi-optical characteristics of atmospheric aerosol.

Keywords: spectroscopy, synchronous detection, coupling spectrum, coupled photoacoustic cavity

PACS: 07.88.+y, 07.60.Rd, 42.60.Da, 43.58.Kr **DOI:** 10.1088/1674-1056/ac43ad

1. Introduction

With the development of society and economy, environmental pollution has been a serious threat to people's physical and mental health. Therefore, it is urgent to understand the mechanism of environmental and atmospheric pollution. Atmospheric aerosol is an important factor affecting atmospheric oxidation,[1] regional pollution transport[2,3] and disease prevention and control.[4,5] It is very important to accurately measure the optical characteristic parameters of atmospheric aerosol, such as extinction coefficient, absorption coefficient and scattering coefficient. These optical characteristics have important effects on atmospheric radiation, environmental protection and occupational disease prevention and control.

In order to accurately detect the optical characteristic parameters of aerosols, the filter technology,[6] cavity ring-down spectrometer (CRDS),[7,8] photoacoustic spectroscopy (PAS),[9,10] cavity enhanced absorption spectroscopy (CEAS),[11,12] and laser induced fluorescence technology (LIF)[13,14] have emerged successively, and the extinction coefficient and absorption coefficient of aerosols have been measured by the above technologies. Among them, Chen *et al.*[15] developed a set of aerosol absorption coefficient measurement system by using photoacoustic spectroscopy technology, and successfully measured the aerosol absorption coefficient of the ambient atmosphere. Liu *et al.*[16] developed an aerosol optical absorption measuring instrument based on photoacoustic spectroscopy. The detection sensitivity of aerosol absorption coefficient at 532 nm reached 1.30 Mm^{-1}. Li *et al.*[17] developed a cavity ring-down spectrometer with a minimum aerosol extinction coefficient of 6.10×10^{-7} Mm^{-1}. In view of the measurement of aerosol optical characteristic parameters, many methods have been used to conducted in-depth research, but most of them are single system of single parameter measurement. However, the existing multi-parameter synchronous detection technologies are greatly affected by sampling loss, cavity difference, detection source, and other factors, and there are technical problems such as inconsistent detection benchmark, unable to make accurate synchronous detection, *etc*.[18] Dial *et al.*[19] proposed an aerosol albedo meter that includes an attenuation chamber and an integrating sphere. The aerosol albedo meter can simultaneously measure the scattering coefficient and extinction coefficient of fixed frequency light, and then the relative measurement uncertainty of single scattering albedo can be obtained. The detection sensitivity of scattering coefficient and extinction coefficient are 2.70 Mm^{-1} and 0.60 Mm^{-1}, respectively. Sharma *et al.*[20] conducted photoacoustic and scattering spectroscopic study of aerosol optical properties, and measured the aerosol absorption and scattering coefficients at five wavelengths (central wavelength 417 nm, 475 nm, 542 nm, 607 nm, and 675 nm). Thompson *et al.*[21] proposed a method of measuring aerosol single scattering albedo at 532 nm, in which mainly cavity ring-down spec-

†Corresponding author. E-mail: rzhu@aiofm.ac.cn
‡Corresponding author. E-mail: phxie@aiofm.ac.cn

© 2022 Chinese Physical Society and IOP Publishing Ltd

trometer was used to measure aerosol extinction coefficient, and also adopted an integrating sphere turbid meter to measure aerosol scattering coefficient. The detection limits of extinction coefficient and scattering coefficient reached 0.61 Mm^{-1} and 2.70 Mm^{-1}, respectively. Ma and Thompson[22] developed an aerosol albedo meter with cavity ring-down spectrometer and integrating sphere, which was used to measure the extinction coefficient and scattering coefficient of particles in the near ultraviolet region.

The above-mentioned synchronous detection methods of optical characteristic parameters mostly involve direct measurement of scattering coefficient using integrating sphere as carrier, or using synchronous measurement of extinction coefficient and scattering coefficient, or absorption coefficient and scattering coefficient. However, there is still room for the improvement in the measurement of scattering coefficient by integrating turbid meter in terms of obtaining light scattering intensity and scattering information. Based on this, a spectroscopic system for the simultaneous measurement of aerosol absorption coefficient and extinction coefficient is developed based on two mature optical cavity techniques: photoacoustic spectroscopy and cavity ring-down spectrometer. In this way, the technical problems of the system sampling can be overcome, such as inconsistent detection benchmark, and failing-to-implement synchronous and accurate detection.

2. Measuring principle

Photoacoustic spectroscopy is a detection method based on photoacoustic effect. When the molecule absorbs the light of P power and forms a heat source with periodic changes, the pressure in the measuring cavity changes periodically, and the sound signal S_{PA} is stimulated. The photoacoustic signal is detected by a microphone (sensitivity S_m), and the cell constant C_{cell} is regarded as the inherent property of the photoacoustic cavity, and its value can be systematically calibrated by an object with a known absorption cross section. Therefore, the absorption coefficient α_{abs} of aerosol can be expressed as[23]

$$\alpha_{abs} = \frac{S_{PA}}{C_{cell} P_0 S_m}. \tag{1}$$

The measurement principle of cavity ring-down spectrometer is based on Lambert Beer's law. Optical resonators (with high reflection mirror seals at both ends) are used to increase the effective absorption path. When the incident light is coupled to the cavity, multiple reflections occur in the cavity, and the light intensity signal after having passed through the optical resonator decays exponentially. According to the length of optical resonator d, sample length L_s, ring-down time τ, background ring-down time τ, and the speed of light c, the relationship between the optical intensity ring-down time and the aerosol extinction coefficient can be established.[24] Therefore, the extinction coefficient α_{ext} of aerosol can be expressed as

$$\alpha_{ext} = \frac{d}{cL_s}\left(\frac{1}{\tau} - \frac{1}{\tau_0}\right). \tag{2}$$

In the actual measurement, the extinction coefficient of the sample with or without aerosol is measured twice, and then the extinction coefficient of the aerosol is calculated from the following formula:

$$\alpha_{ext_aerosol} = \alpha_{ext_have\ aerosol} - \alpha_{ext_no\ aerosol}. \tag{3}$$

The absorption coefficient and extinction coefficient of aerosol can be detected by the coupled measurement spectral system, and then the aerosol scattering coefficient α_{scat} and single scattering albedo ω can be deduced from the following formulae:[25]

$$\alpha_{scat} = \alpha_{ext} - \alpha_{abs}, \tag{4}$$

$$\omega = \frac{\alpha_{scat}}{\alpha_{ext}} = \frac{\alpha_{ext} - \alpha_{abs}}{\alpha_{ext}}. \tag{5}$$

3. Design of coupling cavity and system

3.1. Design of three-stage coupling cavity

The system of synchronously measuring the atmospheric aerosol absorption coefficient and extinction coefficient is mainly based on the coupling optical cavity composed of photoacoustic spectroscopy and cavity ring-down spectrometer. It adopts the same light source, optical path, gas path, frequency modulation, timing sequence and cavity. In this work, a three-stage coupling cavity is designed, which is respectively composed of two sections of thin aluminum tubes and one section of thick aluminum tube connected end to end as shown in Fig. 1. The thick aluminum tube is located in the middle, and two sections of thin aluminum tube are located at both ends. Purge holes and inlet and outlet holes are respectively arranged on the thin aluminum tube to construct the sampling air path of the system.

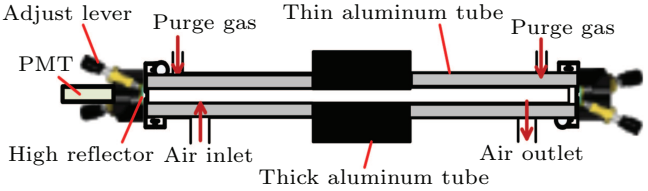


Fig. 1. Three-stage coupled cavity.

The specific parameters of the three-stage cavity are shown in Table 1. The inner hole of the aluminum tube is uniform in size, specifically, 8 mm, which matches the beam diameter, and the overall length of the cavity after connection is 780 mm. Both ends of the optical resonator are equipped with high reflection mirror adjustment frame, which can not only adjust the high reflection mirror, but also support and fasten the photomultiplier tube (PMT). When adjusting the light

path, the laser passes through the center of the high reflection mirror by adjusting the adjusting knob and the fixing screw, so as to achieve the effect of maximum reflection times. The maximum number of reflections is determined by measuring the residual light intensity with a photomultiplier tube and then fitting the ring-down curve.

Table 1. Cavity parameters of coupling spectral measurement system.

Name	Number	Length (mm)	Radius (mm)	Location	Cavity material
Resonator cavity	1	120	8	middle	aluminum
Buffer cavity	2	330	25	side	aluminum

3.2. Influence of buffer cavity on coupling photoacoustic system

Compared with the photoacoustic cavity, the coupling cavity has a length that is increased to match the cavity length of the cavity ring-down system. In order to study the influence of 330 mm buffer cavity on the coupling measurement system, an acoustic finite element model of the coupling cavity is established, and its simulation cloud image (the cavity was set as nitrogen) is obtained as shown in Fig. 2. From the simulation results of the sound field distribution in the cavity, it can be seen that the middle part of the resonator cavity is the acoustic maximum position, and the sound pressure value decreases along the axis to both ends of the resonator cavity, and the closer to the two ends of the photoacoustic cell, the lower the sound pressure value is. It can be seen that the established coupling cavity has little influence on the sound field distribution of the photoacoustic system, and the microphone should be placed in the middle of the resonator cavity to collect the sound signal during measurement.

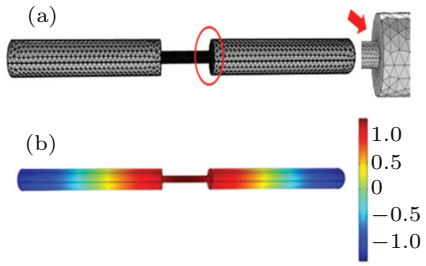


Fig. 2. Coupled cavity acoustic mesh model and simulation cloud map: (a) coupled cavity finite element model, and (b) cloud image of coupling cavity acoustic simulation.

3.3. Design of coupling measurement spectrum system

The coupling measurement spectral system designed in this paper is shown in Fig. 3, which mainly includes 405-nm blue diode laser (DL-405), coupling measurement cavity, signal processing module and gas path system. The system is purged by pure nitrogen to protect the high reflection mirror, and the purging flow rate is 50 mL/min. The interference of large particles in the ambient atmosphere is filtered with a filter membrane, and the flow rate is controlled by a mass flow meter (CS200) to be 0.5 L/min. The ambient air is pumped into the coupling chamber by means of a small pump (N83KNE). The square wave modulated diode laser outputs 405 nm blue light at a specific frequency, which is reflected by the mirror and then enters into the coupling measurement cavity. The acoustic signal and light intensity signal of the coupled photoacoustic cavity are detected by microphone (MP201) and photomultiplier tube (H10721-210) respectively. The LabVIEW software collects the ring-down signal of light intensity output from photomultiplier tube in real time, and the lock-in amplifier (OE1022D) detects the signal of microphone in real time. The time constant of the PLL amplifier is set to be 3 s, the sensitivity 200 μV, the attenuation rate 12 dB, and the sampling time 1000 ms.

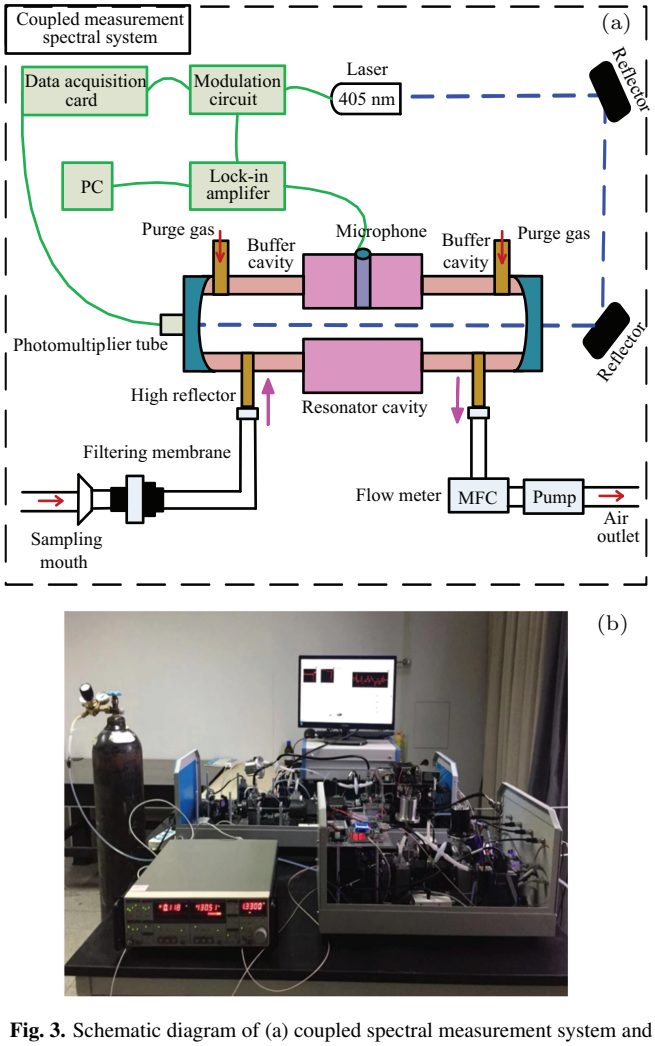


Fig. 3. Schematic diagram of (a) coupled spectral measurement system and (b) real picture of coupled spectral measurement system.

4. Experimental results and discussion

4.1. Calibration of system

Because the aerosol has no obvious absorption peak, the NO_2 gas with known absorption cross section is used to calibrate the system. However, NO_2 gas molecules have a strong absorption peak near 403 nm, and water vapor and other interfering gases have no obvious absorption near 403 nm. Therefore, the 405 nm blue diode laser with rated power of 120 mW is selected as an excitation source of the system in this paper. By accurately controlling the mass flowmeter, 7 mg/m^3NO_2 is diluted into 19.20 μg/m^3, 48.10 μg/m^3, 92.20 μg/m^3, 192.50 μg/m^3, 384.90 μg/m^3, and 577.40 μg/m^3, respectively, and then passed into the system at a flow rate of 200 mL/min to record the value of photoacoustic signal. Combined with the specific absorption coefficient of NO_2 studied by Sharma *et al.*[20] under the experimental conditions (293 K, 101.325 kPa), the specific absorption coefficient of NO_2 is 195.28 Mm^{-1}·(mg·m^{-3})$^{-1}$, and then the calibration curve of the system can be obtained (pink line in Fig. 4). The slope after calibration curve fitting is 0.04368 μV/Mm^{-1}, and R^2 is 0.998. According to Eq. (1), the constant number of cell is 300.24 Pa·cm·W^{-1}. According to the Allan analysis of variance (red line in Fig. 4) of the system, the detection limit of absorption coefficient of the coupling photoacoustic spectrum system is 0.45 Mm^{-1} in an average time of 1 min.

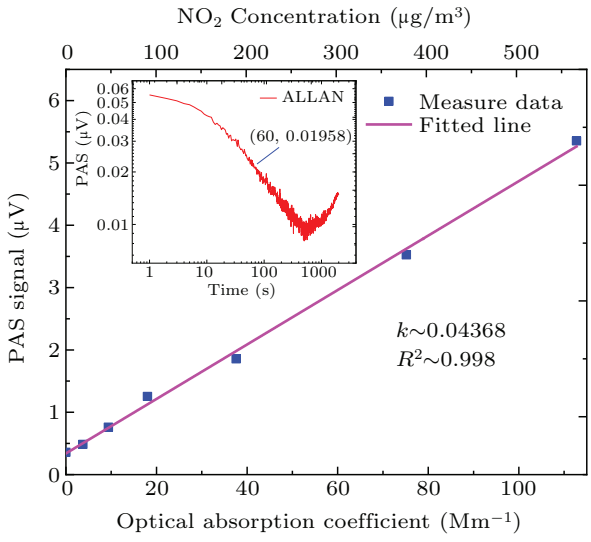


Fig. 4. Calibration study.

For the coupling ring-down cavity, since the cavity length d is 780 mm and the sample length L_s is 695 mm, so the ratio R_L is 1.122. At a sampling frequency of 2.5 M, the ring-down time τ_0 is 11.436 μs, then the lowest detection limit of the coupled ring-down cavity is

$$[A]_{\min} = \frac{R_L}{c\sigma}\frac{(\tau_0-\tau)_{\min}}{\tau_0^2} \approx \frac{R_L}{c\sigma}\frac{\sqrt{2}\sigma(\tau_0)}{\tau_0^2} = 0.93 \text{ ppb}. \quad (6)$$

The gradient test results of the coupled ring-down cavity are shown in Fig. 5. When standard sample gas separately with a volume fraction of 41.36 ppb, 90.18 ppb, 141.07 ppb and 192.25 ppb are introduced, the corresponding fluctuation of detected concentration separately is 0.63 ppb, 0.62 ppb, 0.85 ppb, and 0.99 ppb. It can be seen that the linear gradient of the coupled ring-down cavity is good, and the correlation R^2 is close to 1. Combined with the experimental conditions (293 K, 101.325 kPa) and Sharma *et al.*'s study on the specific absorption coefficient of NO_2, it can be seen that the specific absorption coefficient of NO_2 is 195.28 Mm^{-1}·(mg·m^{-3})$^{-1}$, so in an average time of 60 s, the detection limit of spectral extinction coefficient of coupling ring-down cavity is 0.11 Mm^{-1}.

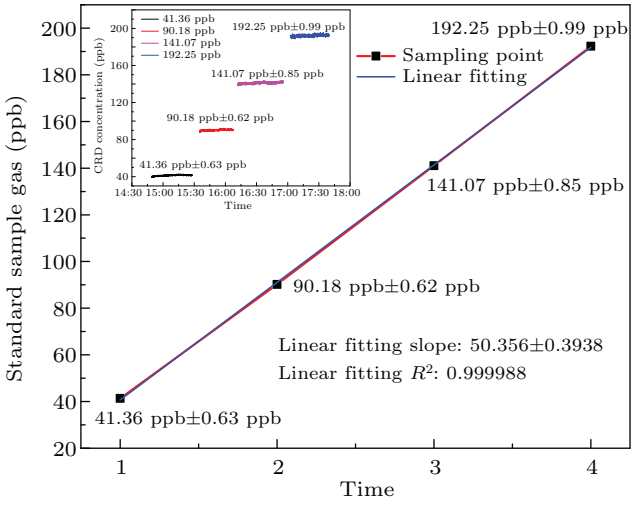


Fig. 5. Ring-down cavity performance analysis.

4.2. Measurement of aerosol absorption coefficient and extinction coefficient

Using the system, we carry out the simultaneous measurement of atmospheric aerosol absorption coefficient and extinction coefficient at Dongpu reservoir (117°16′ longitude, 31°90′ latitude) in Hefei from December 10 to 31, 2019. The measurement results are shown in Fig. 6. From December 15, 2019 to December 29, 2019, due to the heavy rain, in order to avoid rain affecting the experimental equipment, the windows were opened but left gaps, and the position of the sampling tube was changed from 1 meter away from the window to 15 cm away from the window, but the measured data during the rain were still environmental atmospheric data. The black line in Fig. 6 shows the aerosol extinction coefficient detected by cavity ring-down spectrometer system. The analysis shows that the aerosol extinction coefficient fluctuated greatly before and after the rainstorm, but the indoor aerosol extinction coefficient fluctuated less during the rainstorm. The overall amplitude ranged from 66.32 Mm^{-1} to 537.87 Mm^{-1}, the average value was 158 Mm^{-1}, and the variance reached 78.89 Mm^{-1}. The red line in Fig. 6 shows the aerosol absorption coefficient measured by the photoacoustic spectrometer system. It can be seen from the analysis that it is relatively stable on the

whole and affected by the rainstorm. Its amplitude range is from 30.90 Mm^{-1} to 111.02 Mm^{-1}, with an average value of 61.70 Mm^{-1} and a variance of 7.71 Mm^{-1}.

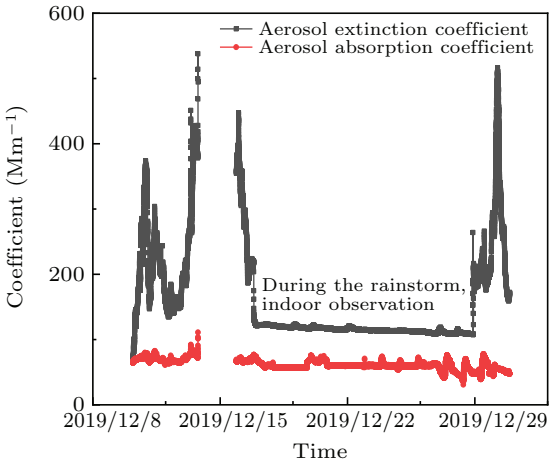


Fig. 6. Time series of aerosol extinction coefficient and absorption coefficient.

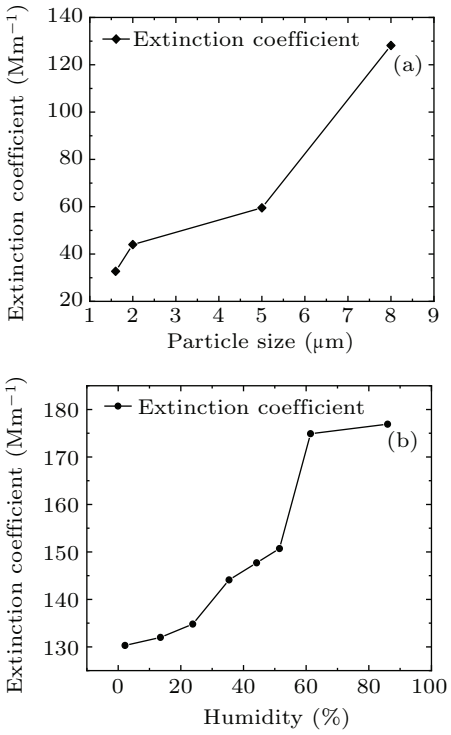


Fig. 7. Influence of particle size and humidity on extinction coefficient: (a) Extinction coefficients of particles with different particle sizes, (b) extinction coefficients at different humidities.

In order to verify the influence of particle size on aerosol extinction coefficient, the relationship between aerosol extinction coefficient and particle size is studied by aerosol generator in laboratory environment. The required liquid is polystyrene microspheres (4205A), whose average diameter of standard microspheres is 5.027 μm±0.047 μm, and the density of microspheres is 1.05 g/cm^3. By selecting generating liquids with different particle sizes, namely 1.6 μm, 2 μm, 5 μm, and 8 μm, and diluting them to specific concentrations by ionic water, the extinction coefficients of particles with different particle sizes at the same concentration are studied, and the results are shown in Fig. 7(a). It can be seen from the figure that the extinction coefficient of particles increases with the increase of concentration. Heavy rain will affect air humidity. In order to further obtain the relationship between humidity and extinction coefficient, we use the humidity control system to investigate the humidity ratios of standard source gas, which are 0%, 13.5%, 23.8%, 35.4%, 44.2%, 51.5%, 61.4%, and 86% respectively. The extinction coefficients under different humidities are observed as shown in Fig. 7(b). As can be seen from the figure, extinction coefficient increases with the increase of humidity.

4.3. Analysis of aerosol single albedo

According to the measured aerosol extinction coefficient and absorption coefficient, the single time series of aerosol albedo can be calculated from Eq. (5), and the results are shown in Fig. 8. According to the figure, the aerosol single albedo during the observation period is relatively stable, ranging from 0.26 to 0.89, with an average of 0.56 and a variance of 0.13. The single albedo was maintained in a low range during the rainstorm, and the minimum value of single albedo was about 0.31 at 23:02 on December 27 2019. At this time, the proportion of aerosol absorption coefficient to extinction coefficient was relatively large, the ability of aerosol to scatter had a relatively large decline, and the air was relatively clean. After the rainstorm, the aerosol single albedo, extinction coefficient and scattering coefficient increased together, and gradually recovered to their values before the rainstorm.

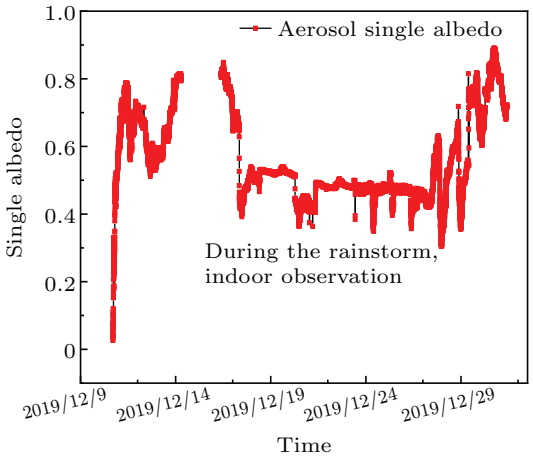


Fig. 8. Time series of aerosol single albedo.

4.4. Relationship between aerosol scattering coefficient and extinction coefficient

According to the measured aerosol extinction coefficient and absorption coefficient, the aerosol scattering coefficient time series during the observation period can be calculated from formula (4), and the results are shown in Fig. 9(a). As can be seen from the figure, the aerosol scattering coefficient

during the observation period fluctuated greatly before and after the rainstorm, the overall amplitude range was 50.40 Mm^{-1} to 459.97 Mm^{-1}, the average value was 96.28 Mm^{-1}, and the variance was 73.54 Mm^{-1}. Figure 9(b) shows the correlation between aerosol extinction coefficient and scattering coefficient during the observation period. As can be seen from the figure, the correlation R^2 between aerosol extinction coefficient and scattering coefficient is 0.990, and the fitting slope is 0.96. It can be seen that the aerosol scattering coefficient contributes greatly to the extinction coefficient during the observation period.

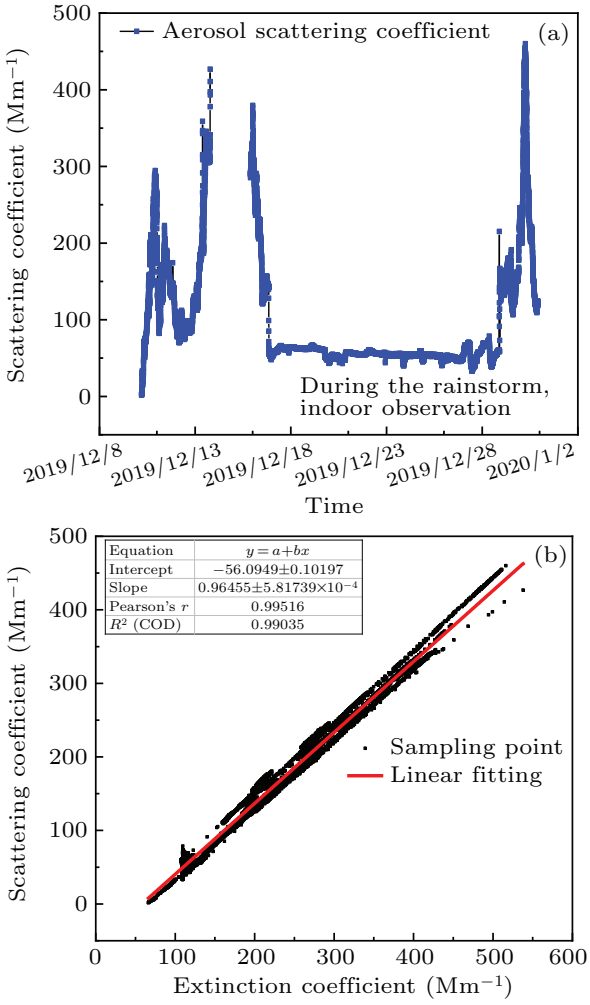


Fig. 9. Aerosol scattering coefficients *versus* (a) time and (b) extinction coefficient.

4.5. Comparative study of data of environmental quality monitoring station

Because the atmospheric aerosol is a multiphase system, the particulate matter has a great influence on it, which can reflect the accuracy of the system detection to a certain extent. In order to understand the contribution of particulate matter to atmospheric aerosol and verify the accuracy of the system, the correlation between particulate matter and atmospheric aerosol extinction coefficient is studied. The monitoring data of PM2.5 and PM10 from the China air pollution quality monitoring station Hefei Dongpu reservoir station (117°16′ longitude, 31°90′ latitude) are adopted. The corresponding aerosol extinction coefficient and PM2.5 mass concentration time series during the observation period are shown in Fig. 10, and the aerosol extinction coefficient and PM10 mass concentration time series during the observation period are shown in Fig. 11.

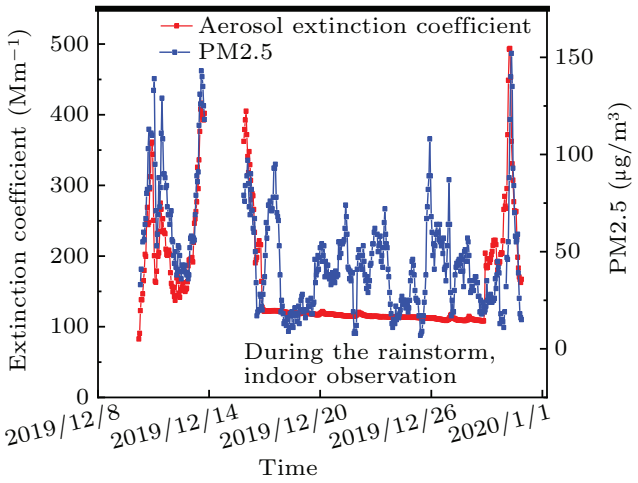


Fig. 10. Time dependence of aerosol extinction coefficient and PM2.5.

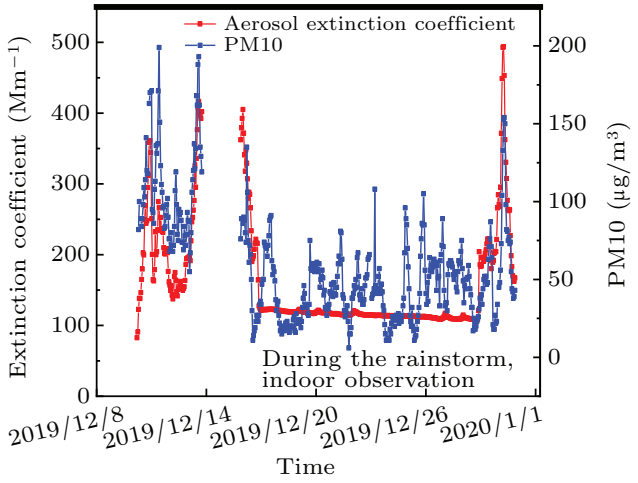


Fig. 11. Time dependence aerosol extinction coefficient and PM10.

According to the figure, the mass concentration of PM2.5 ranges from 7 μg/m^3 to 152 μg/m^3, the average value is 49.05 μg/m^3 and the variance is 27.98 μg/m^3. The mass concentration of PM10 is in a range from 11 μg/m^3 to 199 μg/m^3, with an average value of 59.74 μg/m^3 and a variance of 34.64 μg/m^3. The variation trend of aerosol extinction coefficient before and after the rainstorm are consistent with those of PM2.5 and PM10, but the sampling difference is large. Therefore, the data before the rainstorm from December 10 to December 14 2019 are selected for correlation study, and the results are shown in Figs. 12 and 13.

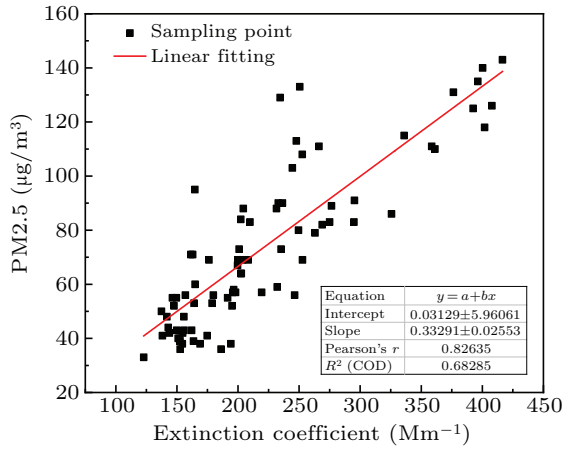


Fig. 12. Variation of PM2 with aerosol extinction coefficient.

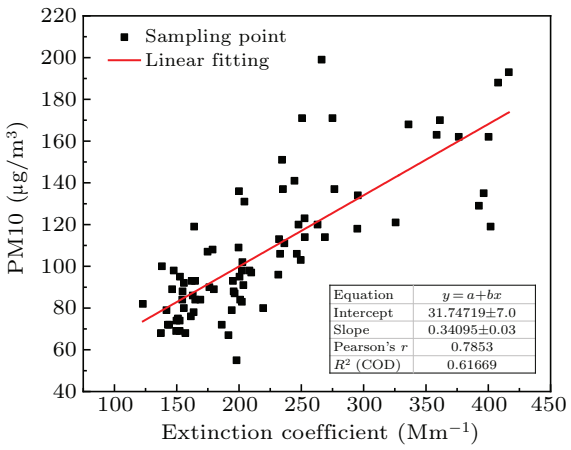


Fig. 13. Variation of PM10 with aerosol extinction coefficient.

As can be seen from Figs. 12 and 13, the correlation R^2 between PM2.5 mass concentration and aerosol extinction coefficient is 0.683, the fitting slope 0.33, and the intercept 0.03. The correlation R^2 between PM10 mass concentration and aerosol extinction coefficient is 0.617, the fitting slope 0.34, and the intercept 31.75. Since PM2.5 and PM10 can reflect the mass concentration of fine particles and coarse particles in the ambient atmosphere during the observation period, the correlation between PM 2.5 and extinction coefficient, and between PM10 and extinction coefficient show that fine particles in the ambient atmosphere contribute more to extinction coefficient than coarse particles during the observation period.

5. Conclusions

Based on therequirements for simultaneous detection of multiple optical characteristics of aerosol, a new method of coupled cavity ring-down spectroscopy with photoacoustic spectroscopy is proposed in this work. The detection limits of photoacoustic spectroscopy absorption coefficient and extinction coefficient of cavity ring-down spectroscopy after coupling are 0.45 Mm^{-1} and 0.11 Mm^{-1}, respectively, which can meet the measurement requirements for atmospheric aerosol. The absorption coefficient and extinction coefficient of atmospheric aerosol are measured directly and the scattering coefficient and single albedo are calculated. Comparing with the data of environmental quality monitoring station, it can be concluded that the mass concentration of particulate matter has a great influence on the aerosol extinction coefficient, and the measurement results of the system prove accurate. This technique provides a new idea for the simultaneous detection of multiple optical characteristics of atmospheric aerosol.

Acknowledgements

Project supported by the Major Project of Natural Science Research in Universities of Anhui Province, China (Grant No. KJ2021ZD0052), the Open Foundation of Key Laboratory of Environmental Optics and Technology of Chinese Academy of Sciences (Grant No. 2009DP1730652020-03), and the Research and Development Project of Wuhu Research Institute of Anhui University of Science and Technology, China (Grant No. ALW2020YF17).

References

[1] Zhe P, Julia L T, John J O, Geoffrey S T and Jose L J 2019 *Atmosph. Chem. Phys.* **19** 813
[2] Hong Q Q, Liu C, Hu Q H, Xing C Z, Tan W, Liu H R, Huang Y, Zhu Y, Zhang J S, Geng T Z and Liu J G 2019 *Atmosph. Res.* **228** 206
[3] Potier E, Waked A, Bourin A, Minvielle F, Pere J C, Perdrix E, Michoud V, Riffault V, Alleman L Y and Sauvage S 2019 *Atmosph. Res.* **223** 1
[4] Paramesh H 2018 *Indian Journal of Pediatrics* **85** 284
[5] Ferrero L, Ritter C, Cappelletti D, Moroni B, Mocnik G, Mazzola M and Lupi A 2019 *Science of the Total Environment.* **686** 452
[6] Leung W F and Choy H F 2018 *Chem. Eng. Sci.* **182** 67
[7] Yang Z H, Yang Y C, Deng L Z and Yin J P 2018 *Chin. Phys. B* **27** 100601
[8] Odame-Ankrah C A and Osthoff H D 2011 *Appl. Spectroscopy* **65** 1260
[9] Gong P, Xie L, Qi X Q, Wang R, Wang H, Cheng M C, Yang H X, Sun F and Li G P 2015 *Chin. Phys. B* **24** 014206
[10] Jin H W, Xie P H, Hu R Z, Huang C C, Lin C and Wang F Y 2020 *Chin. Phys. B* **29** 060701
[11] Wang H C, Chen J and Lu K D 2017 *Atmosph. Measur. Techniq.* **10** 1465
[12] Aalto A, Genty G, Laurila T and Toivonen J 2015 *Opt. Express* **23** 25225
[13] Wan S, Torkashvand B, Haber T, Suntz R and Deutschmann O 2020 *Appl. Catalysis B-Environmental* **264** 118473
[14] Wang F Y, Hu R Z, Chen H, Xie P H, Wang Y H, Li Z Y, Jin H W, Liu J G and Liu W Q 2019 *Opt. Express* **27** A419
[15] Chen J, Qian X M, Liu Q, Zheng J J, Zhu W Y and Li X B 2020 *Spectroscopy and Spectral Analysis* **40** 2989
[16] Liu Q, Huang H H, Wang Y, Wang G S, Cao Z S, Liu K, Chen W D and Gao X M 2014 *Chin. Phys. B* **23** 228
[17] Li L, Chen J M, Chen H, Yang X, Tang Y and Zhang R Y 2011 *Journal of Aerosol Science* **42** 277
[18] Zhao W X, Xu X Z, Fang B, Zhang Q L, Qian X D, Wang S and Liu P 2017 *Appl. Opt.* **56** E16
[19] Dial K D, Hiemstra S and Thompson J E 2010 *Anal. Chem.* **82** 7885
[20] Sharma N, Arnold I J, Moosmuller H, Arnott W P and Mazzoleni C 2013 *Atmosph. Measur. Techniq.* **6** 3501
[21] Thompson J E, Barta N, Policarpio D and DuVall R 2008 *Opt. Express* **16** 2191
[22] Ma L L and Thompson J E 2012 *Anal. Chem.* **84** 5611
[23] Li Z Y, Hu R Z, Xie P H, Chen H, Liu X Y, Liang S X, Wang D, Wang F Y, Wang Y H, Lin C, Liu J G and Liu W Q 2019 *Atmosph. Measur. Techniq.* **12** 3223
[24] Li Z Y, Hu R Z, Xie P H, Wang H C Lu K D and Wang D 2018 *Science of The Total Environment* **613–614** 131
[25] Jin H W, Hu R Z, Xie P H, Huang C C, Wang F Y and Lin C 2020 *IEEE Photon. J.* **12** 1